nature cell biology

AKAP-Lbc enhances cyclic AMP control of the ERK1/2 cascade

F. Donelson Smith[1], Lorene K. Langeberg[1], Cristina Cellurale[2], Tony Pawson[3], Deborah K. Morrison[4], Roger J. Davis[2] and John D. Scott[1,5]

Mitogen-activated protein kinase (MAPK) cascades propagate a variety of cellular activities[1]. Processive relay of signals through RAF–MEK–ERK modulates cell growth and proliferation[2,3]. Signalling through this ERK cascade is frequently amplified in cancers, and drugs such as sorafenib (which is prescribed to treat renal and hepatic carcinomas) and PLX4720 (which targets melanomas) inhibit RAF kinases[4,5]. Natural factors that influence ERK1/2 signalling include the second messenger cyclic AMP[6,7]. However, the mechanisms underlying this cascade have been difficult to elucidate. We demonstrate that the A-kinase-anchoring protein AKAP-Lbc and the scaffolding protein kinase suppressor of Ras (KSR-1) form the core of a signalling network that efficiently relay signals from RAF, through MEK, and on to ERK1/2. AKAP-Lbc functions as an enhancer of ERK signalling by securing RAF in the vicinity of MEK1 and synchronizing protein kinase A (PKA)-mediated phosphorylation of Ser 838 on KSR-1. This offers mechanistic insight into cAMP-responsive control of ERK signalling events.

ERK cascades couple signals from growth factors to cell proliferation through mobilization of the GTPase Ras. Active Ras stimulates RAF kinase, which in turn phosphorylates and activates MEK. This intermediary enzyme relays the signal by phosphorylating the terminal kinase ERK, which as an effector enzyme then acts on a range of downstream targets. Interest in this signalling pathway has been prompted by clinical evidence that activating mutations in Ras are found in 20–25% of all human tumours[8]. Second messengers, such as cAMP, can alter signalling through this pathway[6,7]. However, the mechanism of cAMP action has been challenging to unravel and engenders controversy[9]. Depending on cell type, cAMP positively or negatively controls ERK1/2 activity. Furthermore, cAMP can function through protein kinase A (PKA)-mediated phosphorylation or through the mobilization of guanine nucleotide exchange factors (Epacs) for the Ras-like small GTPases Rap1 and Rap2 (refs 10, 11). As A-kinase anchoring proteins (AKAPs) compartmentalize PKA and Epacs[12], we hypothesized that AKAPs could contribute to the modulation of the ERK cascade.

AKAP-Lbc functions as a guanine nucleotide exchange factor for small GTPases and as a kinase-anchoring protein[13,14]. We performed a proteomic screen for binding partners that could affect ERK1/2 signalling. Lysates from HEK293 cells expressing epitope-tagged (Flag) AKAP-Lbc were incubated with anti-Flag antibodies, immunoprecipitated complexes were isolated and separated by SDS–PAGE and associated proteins were identified by tandem (MS/MS) mass spectrometry (Fig. 1a). Detection of peptides from AKAP-Lbc and regulatory (RII) and catalytic subunits of PKA (PKAc) were used as internal controls. Peptides from KSR-1, a scaffolding protein for members of the RAF–MEK–ERK cascade[15], were also identified (Fig. 1a).

This protein–protein interaction was validated in HEK293 cells when recombinant KSR-1 was detected in AKAP-Lbc immunoprecipitated complexes (Fig. 1b). NIH3T3 fibroblasts endogenously express AKAP-Lbc and KSR-1. Accordingly, native AKAP-Lbc was co-purified in complex with haemagglutinin (HA)-tagged KSR-1 from the lysates of NIH3T3 fibroblasts expressing HA–KSR-1 (Fig. 1c), and the native proteins were found to interact when AKAP-Lbc was immunoprecipitated from the lysates of NIH3T3 cells (Fig. 1d). KSR-1 immunoprecipitated complexes also contained both RII and C subunits of PKA (Fig. 1e). Next, mapping studies were used to define the interactive surfaces on both AKAP-Lbc and KSR-1 (Fig. 1f–j). Binding of KSR-1 to a family of immobilized GST–AKAP-Lbc fragments detected direct interaction with a central portion of AKAP-Lbc (residues 1388–1922; Fig. 1g, h). Reciprocal experiments demonstrated that AKAP-Lbc interacts with the 331 carboxy-terminal residues of KSR-1 (Fig. 1i, j). We wanted to investigate how AKAP-Lbc affects KSR-1 function further, especially because cAMP exerts pleiotropic effects on the ERK cascade[11].

Dynamic changes in ERK activity were measured with a genetically encoded fluorescence based Erk-kinase-activity reporter (EKAR)[16]. Phosphorylation of a consensus MAPK-target sequence in the reporter promotes Förster resonance energy transfer (FRET). Changes in the

[1]Howard Hughes Medical Institute, Department of Pharmacology, University of Washington School of Medicine, 1959 Pacific Avenue NE, Seattle, WA 98195, USA. [2]Howard Hughes Medical Institute, University of Massachusetts, Program in Molecular Medicine, 373 Plantation Street Worcester, MA 01605, USA. [3]Samuel Lunenfeld Research Institute, Mount Sinai Hospital, 1084-600 University Avenue, Toronto, Ontario, M5G 1X5, Canada. [4]Laboratory of Cell and Developmental Signalling, NCI-Frederick, Building 560, Room 22-90B, Frederick, MD 21702, USA. [5]Correspondence should be addressed to J.D.S. (e-mail: scottjdw@u.washington.edu)

Received 15 April 2010; accepted 13 October 2010; published online 21 November 2010; DOI: 10.1038/ncb2130

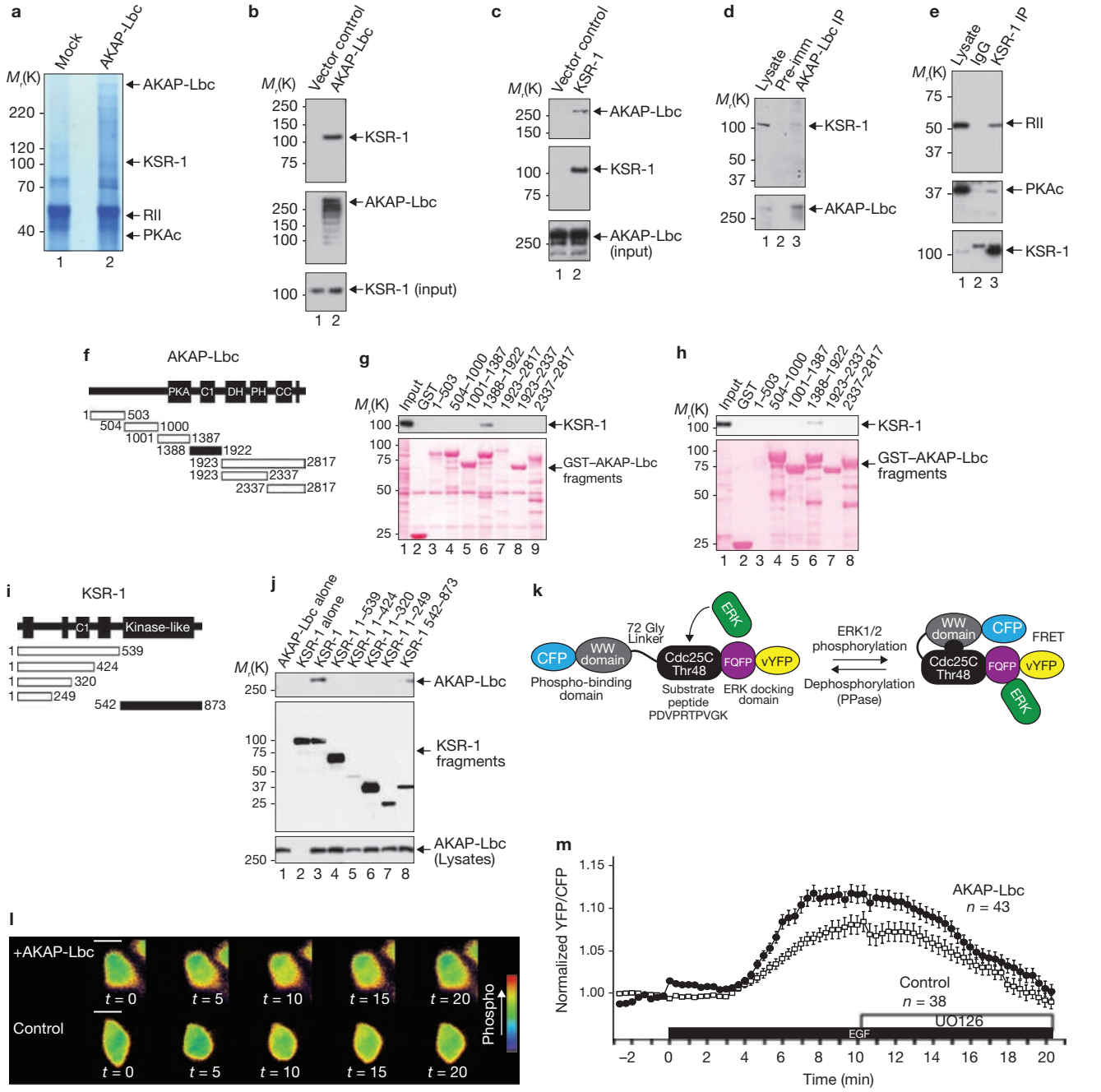

Figure 1 Characterization of AKAP-Lbc–KSR-1 interactions. (**a**) Lysates from HEK293 cells transfected with empty vector or a plasmid encoding Flag-AKAP-Lbc were subject to immunoprecipitation (IP) with anti-Flag antibodies. Proteins were resolved by SDS–PAGE and Coomassie staining, and identified by MS/MS spectrometry. (**b**) Lysates from HEK293 cells expressing HA–KSR-1, and transfected with control vector or vector encoding Flag–AKAP-Lbc, were immunoprecipitated using anti-Flag and proteins were identified by immunoblotting. (**c**) NIH3T3 cells were transfected with control vectors or vectors encoding HA–KSR-1. Cell lysates were immunoprecipitated with anti-HA, and indicated proteins were identified by immunoblotting. (**d**) NIH3T3 lysate and pre-immune or anti-AKAP-Lbc immunoprecipitates were immunoblotted with antibodies against KSR-1 (top) and AKAP-Lbc (bottom). (**e**) NIH3T3 lysate and control immunoglobulin G (IgG) or anti-AKAP-Lbc immunoprecipitates were immunoblotted with antibodies against the indicated proteins. (**f**) Schematic representation of AKAP-Lbc fragments used to construct GST fusion proteins for the pulldown experiments. Shaded fragment indicates KSR-1-binding fragment, as determined in **g** and **h**. (**g**) GST–AKAP-Lbc fragments were used as bait in pulldown experiments using HEK293 lysates. KSR-1 binding was detected by immunoblot (top). GST fusion proteins were resolved by SDS–PAGE and Ponceau S staining (bottom). (**h**) GST–AKAP-Lbc fragments were used as bait in pulldown experiments with *in vitro*-translated recombinant KSR-1. KSR-1 binding was detected by immunoblot (top). GST-fusion proteins were resolved by SDS–PAGE and Ponceau S staining (bottom). (**i**) Schematic representation of KSR-1 fragments used in **j**. Shaded fragment indicates AKAP-Lbc-binding fragment as determined in **j**. (**j**) Pyo-tagged KSR-1 fragments were co-expressed with Flag–AKAP-Lbc in HEK293 cells. Complexes were immunoprecipitated with anti-Pyo. Proteins were detected by immunoblotting with antibodies against the indicated proteins. (**k**) Schematic representation of EKAR, a FRET-based reporter for ERK activity[16]. (**l**) Time-lapse microscopy images of FRET signals in HEK293 cells expressing EKAR alone (bottom), or with AKAP-Lbc–mCherry (top), at indicated times after addition of EGF (min). Scale bars, 10 μm. (**m**) Quantification of normalized YFP/CFP ratio from a FRET experiment as performed in **l**. Black and white bars indicate addition of EGF and UO126, respectively. Uncropped images of blots are shown in Supplementary Information, Fig. S7.

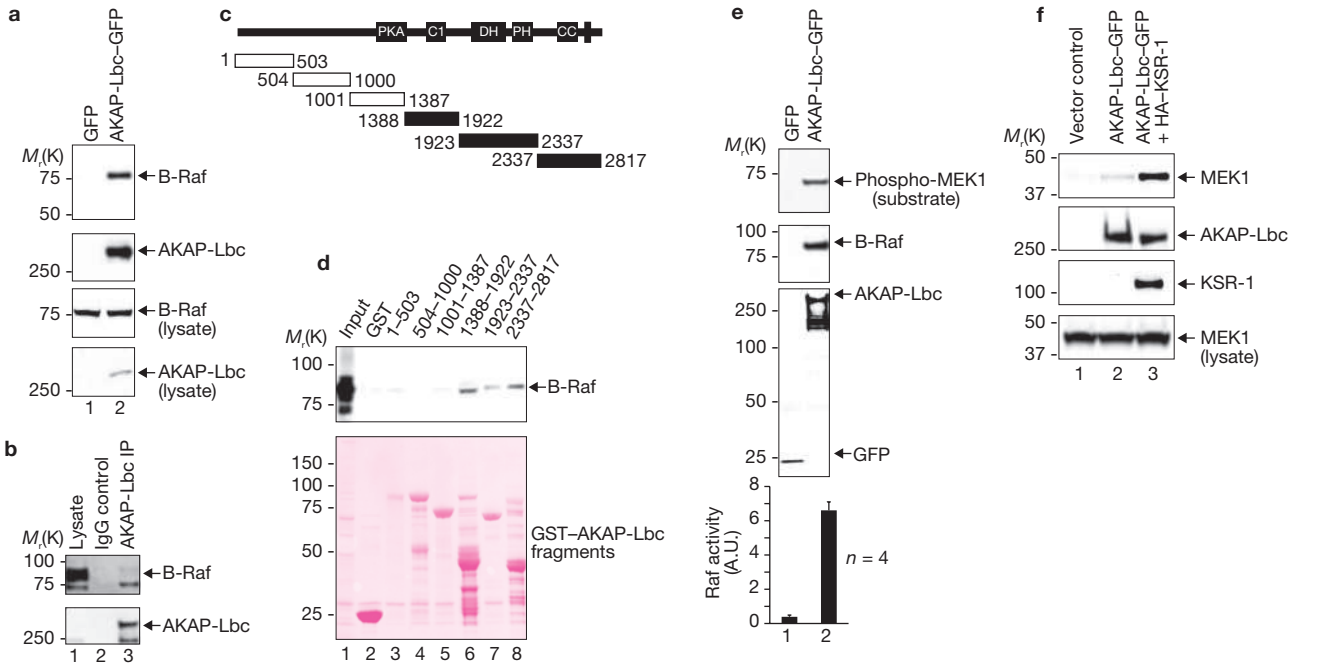

Figure 2 AKAP-Lbc anchors RAF. (**a**) Lysates from HEK293 cells expressing B-Raf and either GFP (left) or AKAP-Lbc–GFP (right) were immunoprecipitated with anti-GFP. The indicated proteins were identified by immunoblotting with antibodies against the indicated proteins. Bottom two panels indicate immunoblot of input lysate. (**b**) NIH3T3 lysate and pre-immune or anti-AKAP-Lbc immunoprecipitates were immunoblotted with antibodies against B-Raf (top) and AKAP-Lbc (bottom). (**c**) Schematic representation of the AKAP-Lbc fragments used to construct GST fusion proteins for the pulldown experiments. Shaded area indicates B-RAF binding fragments, as determined in **d**. (**d**) GST–AKAP-Lbc fragments were used as bait in pulldown experiments using *in vitro*-translated B-Raf. B-Raf binding was detected by immunoblot (top). GST-fusion proteins were resolved by SDS–Page and Ponceau S staining (bottom). (**e**) Cells were transfected, and lysates were immunoprecipitated, as in **a**. The immunoprecipitated complexes were then used in a kinase assay, with kinase-inactive GST–MEK1 as a substrate. Top: immunoblot of kinase assay, using antibodies against the indicated proteins. MEK1 phosphorylation was assessed with antibodies specific to MEK phosphorylated at Ser 218 and Ser 222. Bottom: the phosphorylated MEK-1 band was quantified by densitometry and normalized to the control cells. Data are means ± s.e.m. A.U.; arbitrary units. (**f**) HEK293 cells were transfected with vectors encoding HA–MEK1 and then co-transfected with vectors encoding AKAP-Lbc–GFP and HA–KSR-1, or empty vector controls, as indicated. Cell lysates were immunoprecipitated with anti-GFP, resolved by SDS–PAGE and immunoblotted with antibodies against MEK1, AKAP-Lbc or KSR-1, as indicated. MEK1 levels in lysates were confirmed by immunoblotting (bottom). Uncropped images of blots are shown in Supplementary Information, Fig. S7.

yellow fluorescent protein (YFP)/cyan fluorescent protein (CFP) ratio reflect real-time fluctuations in ERK activity (Fig. 1k). The EKAR signal was detected within 4.3 ± 0.6 min on treatment of control HEK293 cells with epidermal growth factor (EGF; n = 38; Figs 1l; bottom, 1m; open squares). Importantly, the rate of this response was increased 1.81-fold in cells that co-express AKAP-Lbc with EKAR (Figs 1l; top, 1m; black circles). UO1026, a selective MEK inhibitor, suppressed the EKAR response (Figs 1l, m). Thus, AKAP-Lbc augments signal transmission through the ERK cascade.

The RAF kinases (A-Raf, B-Raf and C-Raf) relay intracellular signals from the proto-oncogene Ras to activate the ERK1/2 cascade[17]. RAF selectively targets MEK, the next kinase in the chain. Although RAF is recruited into the KSR-1–MEK–ERK scaffold on growth-factor stimulation,[18] we hypothesized that additional mechanisms might maintain RAF in proximity to its substrate, MEK. Therefore, we tested if RAF kinases interact with AKAP-Lbc. Initially, we investigated B-Raf binding in HEK293 cells expressing epitope (Flag)-tagged B-Raf and detected complexes by immunoprecipitation (Fig. 2a). Native AKAP-Lbc–B–Raf complexes were also isolated from NIH3T3 cells (Fig. 2b), and AKAP-Lbc was found to associate with C-Raf or an oncogenic B-Raf^{V600E} mutant (Supplementary Information, Fig. S1). Recombinant *in vitro*-translated B-Raf was used to screen GST–AKAP-Lbc fragments for direct protein–protein interactions (Fig. 2c, d). GST pulldowns and immunoblot analysis revealed three RAF-binding fragments in the C-terminal portion of AKAP-Lbc (Fig. 2d), suggesting that RAF contacts multiple sites on the anchoring protein. The proximity of these regions to the KSR-1 binding site raised the possibility that KSR-1 and AKAP-Lbc could function cooperatively to recruit RAF. This concept was supported by data indicating that co-expression of B-Raf, KSR-1 and AKAP-Lbc augments formation of a ternary complex (Supplementary Information, Fig. S2a).

Immune-complex kinase assays using inactive MEK1 as a substrate demonstrated that AKAP-Lbc anchors active B-Raf (Fig. 2e). Quantification of phosphorylated MEK indicated a 10.4 ± 0.5-fold (n = 4) enrichment of AKAP-Lbc-associated B-Raf activity when compared with controls (Fig. 2e, bottom). Supplementary experiments confirmed the specificity of this assay (Supplementary Information, Fig. S2b). These results suggest that AKAP-Lbc compartmentalizes RAF in proximity to its substrate. This was supported by experiments whereby co-expression of KSR-1 with AKAP-Lbc enriched the co-purification of MEK1 in AKAP-Lbc-immunoprecipitated complexes (Fig. 2f). These data suggest that AKAP-Lbc and KSR-1 form the core of a signalling network to efficiently relay signals from RAF, through MEK, and on to ERK1/2.

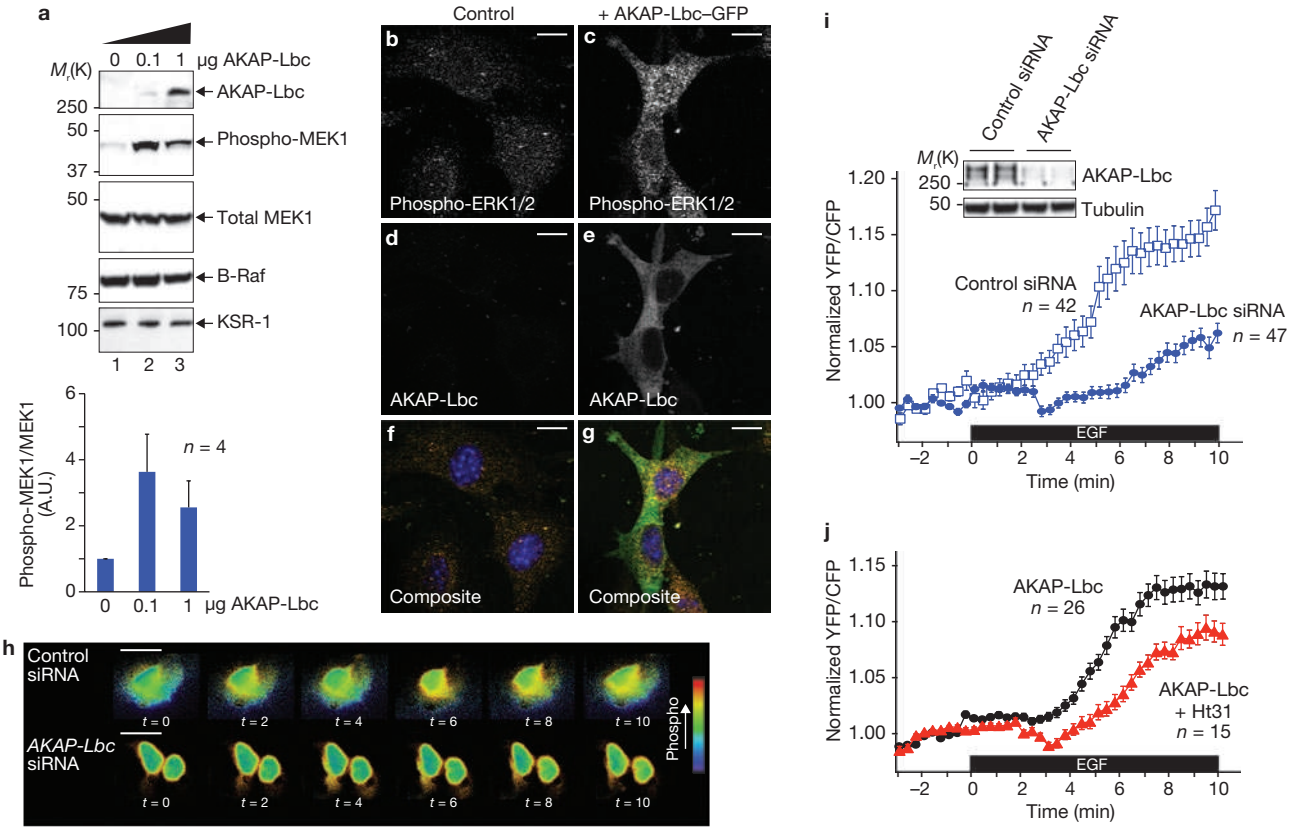

Figure 3 AKAP-Lbc enhances signal relay through the ERK kinase cascade. (**a**) HEK293 cells were transfected with vectors encoding HA–MEK1 and Flag–B-Raf along with increasing amounts of plasmid encoding AKAP-Lbc–GFP. Top: immunoblot of cell lysates used to detect the indicated proteins. Bottom: quantification of the phosphorylated MEK1 band (relative to total MEK) by densitometry (data are means ± s.e.m.). (**b**–**g**) NIH3T3 cells were transfected with a vector encoding AKAP-Lbc–GFP (right) or control vector (left). Cells were fixed and immunostained with antibodies against phosphorylated ERK1/2 (**b**, **c**), or GFP fluorescence was observed (**d**, **e**). **f** is a merge of **b** and **d**, and **g** is a merge of **c** and **e**; in both DAPI was used as a nuclear marker. Scale bars, 20 µm. (**h**) Time-lapse microscopy images of FRET signals in HEK293 cells expressing EKAR and transfected with control siRNA oligonucleotides (top) or siRNA oligonucleotides against AKAP-Lbc, at indicated times after addition of EGF (min). Scale bars, 20 µm. (**i**) Quantification of normalized YFP/CFP ratio from a FRET experiment as performed in **h**. Black bar indicates addition of EGF. Data are means ± s.e.m. Inset: immunoblot of lysates from cells transfected with control or AKAP-Lbc siRNA. (**j**) HEK293 cells were transfected with vectors expressing EKAR and AKAP-Lbc–mCherry. Cells were pre-treated with Ht31 peptide (red) or vehicle as a control (black) before treatment with EGF and FRET recording. Normalized YFP/CFP ratios are indicated. Data are means ± s.e.m. Uncropped images of blots are shown in Supplementary Information, Fig. S7.

To test this hypothesis, we first investigated whether varying the cellular levels of this anchoring protein influenced the basal activation state of MEK, as AKAP-Lbc constitutively binds B-Raf (Fig. 2). Antibodies against phosphorylated MEK1 were used to monitor MEK activation in HEK293 cells (Fig. 3a). The phosphorylated MEK1 signal was hardly detected in control cells, but low-level expression of the anchoring protein (by transfection of cells with 0.1 µg of AKAP-Lbc plasmid) enhanced detection of phosphorylated MEK1 (Fig. 3a). Thus, spatially constraining RAF in the context of the AKAP-Lbc–KSR-1 network favours the relay of signals to MEK. Conversely, high-level expression of AKAP-Lbc (by transfection with 10-fold more plasmid) yielded only a moderate increase in MEK1 phosphorylation (Fig. 3a). Similar results were obtained when antibodies against phosphorylated ERK were used to monitor the activation state of this kinase (Supplementary Information, Fig. S3). This is consistent with the model that a scaffolding protein, if present in excess of its constituent binding partners, impairs signalling by assembling non-productive complexes[19–21].

Detection of phosphorylated ERK1/2 by immunofluorescence microscopy functions as an index of ERK-kinase activation *in situ*[22]. Phosphorylated ERK1/2 staining was barely detectable in control NIH3T3 fibroblasts (Fig. 3b, d, f). However, the basal phosphorylated ERK1/2 signal was enhanced in cells that express recombinant AKAP-Lbc (tagged with GFP for detection in microscopy, Fig. 3c, e, g). These data suggest that the AKAP-Lbc–KSR-1 network maximizes the relay of signals from RAF to ERK in the resting state.

Next, we monitored ERK-activation dynamics on gene silencing of AKAP-Lbc in HEK293 cells. Knockdown of AKAP-Lbc was confirmed by immunoblotting (Fig. 3i, inset). Real-time imaging of cells expressing EKAR demonstrated that depletion of AKAP-Lbc inhibited the onset, and almost abolished, EGF-dependent ERK activation when compared with cells treated with control siRNA (Fig. 3h, i). Additional experiments focused on the contribution of anchored PKA in this process. Global disruption of PKA anchoring is often achieved by the delivery of Ht31, an anchoring-inhibitor peptide derived from AKAP-Lbc[23]. Displacement of PKA on treatment of cells with Ht31 delayed the onset of EGF-mediated EKAR FRET (Fig. 3j, red triangles) when compared with controls (Fig. 3j, black circles). Thus, AKAP-Lbc-directed PKA phosphorylation of substrates within the network may enhance ERK1/2 signalling.

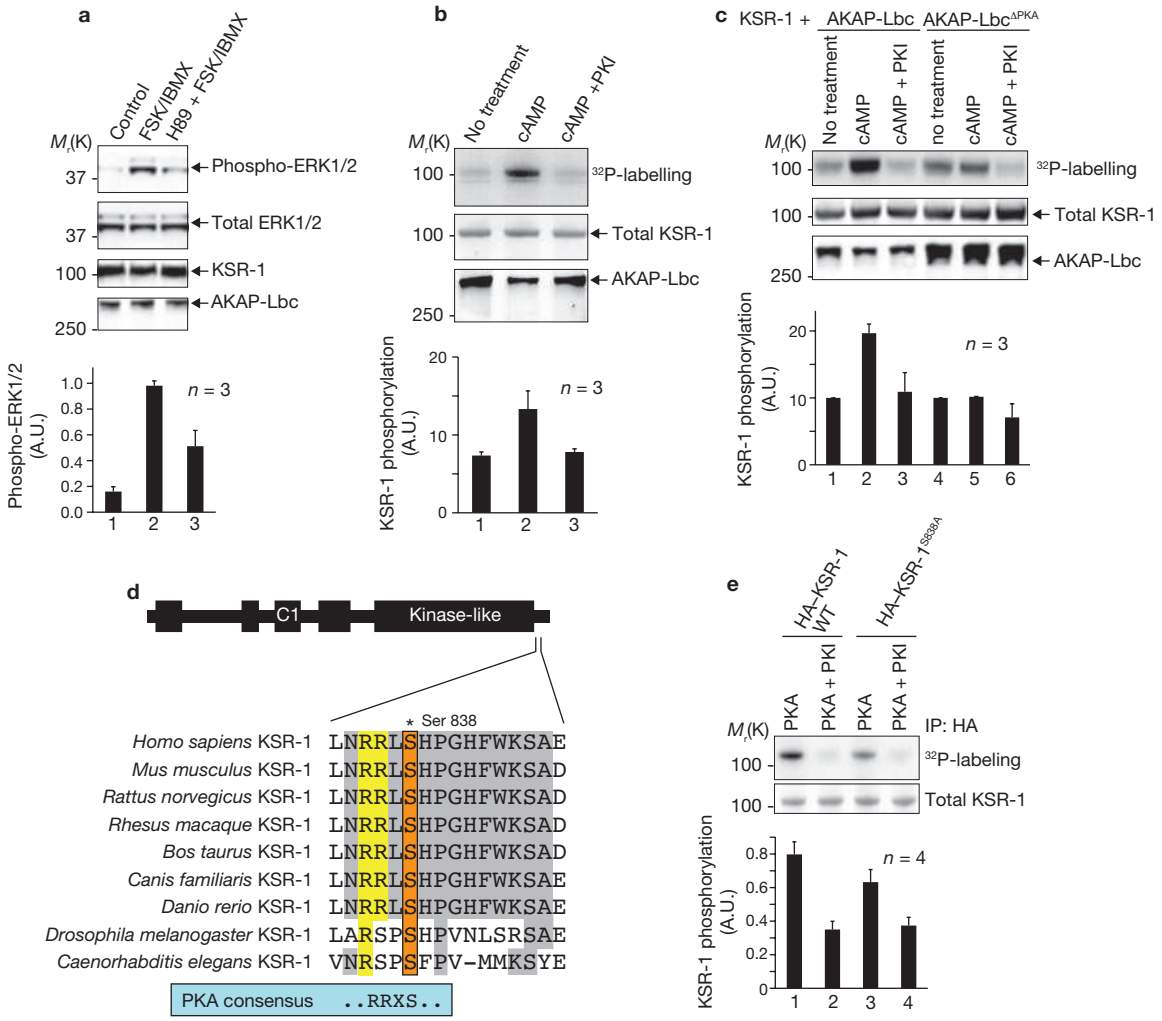

Figure 4 PKA phosphorylation of KSR-1. (**a**) A plasmid encoding KSR-1 was transfected into HEK293 cells, and cells were treated with forskolin and IBMX, and H-89, as indicated. Top: cell lysates were immunoblotted with antibodies against the indicated proteins. Bottom: ERK1/2 activation was measured by quantification of the phosphorylated ERK1/2 bands by densitometry. Values were normalized to total ERK1/2 levels. Data are means ± s.e.m. (**b**) Lysates from HEK293 cells expressing HA–KSR-1 were immunoprecipitated with anti-HA. Top: autoradiograph of immunoprecipitated complexes incubated with [γ-^{32}P] ATP. Immunoprecipitates were also incubated with cAMP and PKI (to block PKA activity) as indicated. Loading controls are also shown. Bottom: bands from the autoradiograph were quantified by densitometry. Data are means ± s.e.m. (**c**) HA–KSR-1 was co-expressed with AKAP-Lbc or AKAP-Lbc$^{\Delta PKA}$ in HEK293 cells. Cell lysates were immunoprecipitated with anti-HA. Top: autoradiograph of immunocomplexes incubated with [γ-^{32}P]ATP, and with cAMP and PKI as indicated. Loading controls are shown. Bottom: bands from the autoradiograph were quantified by densitometry. Data are means ± s.e.m. (**d**) Sequence alignment of a conserved consensus PKA phosphorylation site in KSR-1. The target serine is indicated. (**e**) Lysates of cells expressing wild-type (WT) KSR-1 or a S838A mutant were immunoprecipitated with anti-HA. Top: autoradiograph of immunocomplexes incubated with [γ-^{32}P]ATP, and with PKA and PKI as indicated. Loading controls are shown. Bottom: bands from the autoradiograph were quantified by densitometry. Data are means ± s.e.m. Uncropped images of blots are shown in Supplementary Information, Fig. S7.

Next, we investigated how AKAP-Lbc associated PKA modulates the ERK1/2 cascade. As an anchoring protein, AKAP-Lbc positions PKA close to important substrates, so potential PKA targets were examined in the AKAP-Lbc–KSR-1 complex. In HEK293 cells, cAMP activates ERK1/2, which was suppressed by approximately 48 ± 9% ($n = 3$) on pre-treatment of cells with H-89, a pharmacological inhibitor of PKA (Fig. 4a). Subsequent analysis detected cAMP-responsive phosphorylation of KSR-1 in immunoprecipitated complexes isolated from HEK293 cells (Fig. 4b). This effect was blocked by PKA inhibition with the PKI_{5-24} peptide (Fig. 4b). A role for AKAP-Lbc was established when the AKAP-Lbc–KSR-1 complex was reconstituted with the recombinant anchoring protein or a PKA anchoring-defective mutant (AKAP-Lbc$^{\Delta PKA}$). Robust cAMP-responsive phosphorylation of KSR-1 was detected in the presence of AKAP-Lbc (Fig. 4c). In contrast, near baseline levels of KSR-1 phosphorylation were detected in complexes formed with AKAP-Lbc$^{\Delta PKA}$ (Fig. 4c). Thus, AKAP-Lbc anchors PKA to favour KSR-1 phosphorylation. KSR-1 contains several phosphorylation sites for basophilic kinases (Supplementary Information, Fig. S4), including a well-conserved consensus PKA site (-R-R-L-S-) surrounding Ser 838 (Fig. 4d). Incorporation of ^{32}P into the KSR-1^{S838A} mutant was reduced approximately 21 ± 3% ($n = 4$), compared with a wild-type control (Fig. 4e). These effects were blocked by PKI (Fig. 4e). This suggests that AKAP-Lbc positions PKA to phosphorylate Ser 838 on KSR-1.

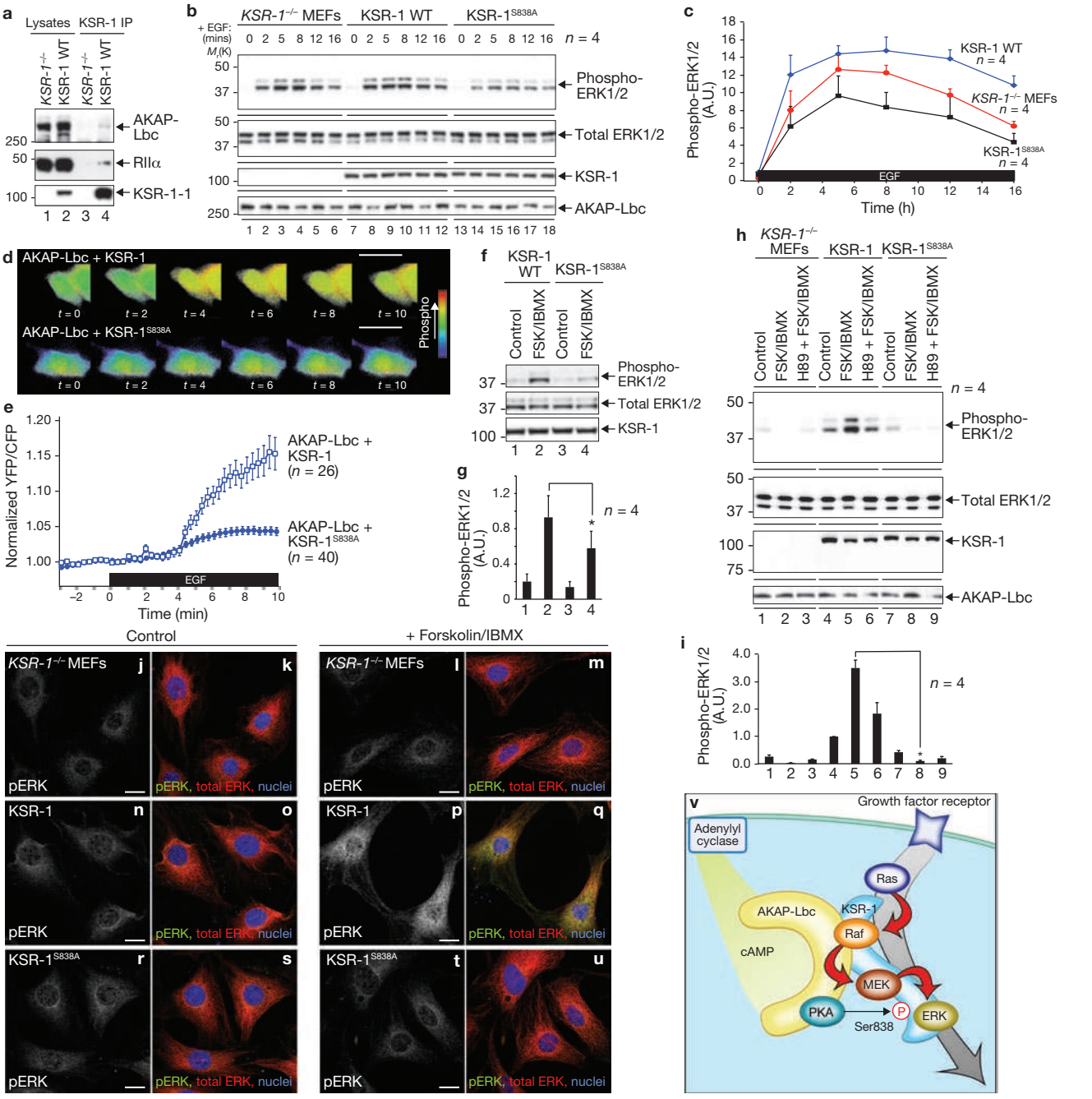

Figure 5 Phosphorylation of KSR-1 on Ser 838 controls ERK1/2 signalling. (**a**) KSR-1 immunoprecipitates from *KSR-1*$^{-/-}$ mouse embryonic fibroblasts (MEFs) and MEFs expressing wild-type KSR-1 were screened for AKAP-Lbc, PKA RII and KSR-1 by immunoblotting. (**b**) Time-course of EGF-stimulated ERK1/2 activity in *KSR-1*$^{-/-}$ MEFs and MEFs expressing wild-type KSR-1 or KSR-1^{S838A}. Starved cells were treated with EGF for the indicated times. ERK activation was assessed by immunoblotting for phosphorylated ERK1/2, ERK1/2, KSR-1 and AKAP-Lbc. (**c**) Quantification of phosphorylated ERK1/2 bands by densitometry, from experiment carried out as in **b** (data are means ± s.e.m.). (**d**) Time-lapse microscopy images of FRET signals in HEK293 cells expressing EKAR, and AKAP-Lbc and wild-type KSR-1 (top), or AKAP-Lbc and KSR-1^{S838A} (bottom), at indicated times after addition of EGF (min). Scale bars, 20 μm. (**e**) Quantification of YFP/CFP ratios for experiment performed as in **d**. Black bar indicates addition of EGF. Data are means ± s.e.m. (**f**) HEK293 cells expressing wild-type KSR-1 or KSR-1^{S838A} were starved and stimulated with forskolin/IBMX, as indicated. ERK activation was measured by immunoblotting of the cell lysates. (**g**) Quantification of phosphorylated ERK1/2 bands by densitometry from experiments performed in **f**. Data are normalized to the density of the total ERK1/2 bands. Data are means ± s.e.m. (asterisk indicates $P < 0.05$, paired *t*-test). (**h**) *KSR-1*$^{-/-}$ MEFs and MEFs expressing wild-type or KSR-1^{S838A} were treated with forskolin and IBMX, and H-89, as indicated. ERK activation was assessed by immunoblotting for phosphorylated ERK1/2, ERK1/2, KSR-1 and AKAP-Lbc. (**i**) Quantification of phosphorylated ERK1/2 bands by densitometry from experiments performed in **h**. Data are normalized to the density of the total ERK1/2 bands. Data are means ± s.e.m. (asterisk indicates $P < 0.001$, ANOVA). (**j–u**) Immunofluorescence microscopy analysis of ERK activation. *KSR-1*$^{-/-}$ MEFs (**j–m**), and MEFs expressing KSR-1 (**n–q**) or KSR-1^{S838A} (**r–u**) were starved, treated with forskolin/IBMX for 10 min, fixed, and immunostained for phosphorylated ERK1/2 and total ERK1/2, as indicated. Scale bars, 20 μm. (**v**) Schematic representation of the AKAP-Lbc–KSR-1 core unit directing growth factor and cAMP signals through the ERK signalling network. Uncropped images of blots are shown in Supplementary Information, Fig. S7.

A more stringent test of this hypothesis was performed with transformed mouse embryonic fibroblast (MEF) cell-lines derived from *KSR-1*$^{-/-}$ animals[24]. As a prelude to these studies, co-immunoprecipitation approaches confirmed that the AKAP-Lbc–PKA complex could be isolated from MEFs expressing wild type KSR-1, but not from *KSR-1*$^{-/-}$ null cells (Fig. 5a). Immunofluorescence microscopy confirmed that the distribution of AKAP-Lbc and KSR-1 overlapped in these cells (Supplementary Information Fig. S5).

Growth-factor-induced ERK1/2 activation was inhibited in *KSR-1*$^{-/-}$ MEFs over a time course of 0–16 min, as assessed by immunoblotting of cell lysates (Fig. 5b, c, red circles). Rescue experiments confirmed that the normal ERK1/2 activation was restored on viral expression of the wild-type scaffolding protein (Fig. 5b, 5c, blue circles). Importantly, the rate and magnitude of growth-factor-induced ERK1/2 activation was inhibited when rescue experiments were performed with the S838A mutant (Fig. 5b, c, black squares). Immunoblot controls confirmed that equal levels of total ERK1/2 and AKAP-Lbc were present and that equivalent amounts of KSR-1 were expressed in the rescued cells (Fig. 5b). Similarly, introduction of KSR-1 supported enhanced ERK activation when the EKAR reporter was used to visualize kinase activity in HEK293 cells (Fig. 5d, e, open squares). However, ERK activation was suppressed in the presence of the KSR-1^{S838A} mutant (Fig. 5d, e, blue circles). Both these approaches suggest that phosphorylation of Ser 838 on KSR-1 ensures optimal activation of the ERK cascade.

Finally, we investigated the impact of the S838A mutation in KSR-1 on cAMP-responsive activation of ERK1/2. cAMP-responsive phosphorylation of ERK1/2 was inhibited (by approximately 30 ± 5%; $n = 4$) in cells expressing the KSR-1^{S838A} mutant, compared with cells expressing wild-type KSR-1 (Fig. 5f, g). Similar analyses in the MEF lines revealed that cAMP stimulation does not result in ERK1/2 activation in *KSR-1*$^{-/-}$ MEFs (Fig. 5h, i). Immunoblotting of lysates from *KSR-1*$^{-/-}$ MEFs that are rescued by re-expression of the wild-type scaffolding protein demonstrates that there is robust ERK1/2 phosphorylation following elevation of cAMP (Fig. 5h, i). In contrast, cAMP stimulation of ERK1/2 activity was not detected in cells rescued with the S838A mutant (Fig. 5h, i). Controls confirmed that equal levels of total ERK1/2 and AKAP-Lbc were present and that equivalent amounts of KSR-1 were expressed in the rescued cells (Fig. 5h). Similar results were obtained when cAMP-responsive ERK1/2 activation was measured over time (Supplementary Information, Fig. S6). Further confirmation of these results was provided by *in situ* immunofluorescence microscopy of phosphorylated ERK1/2 (Fig. 5j–u). These results suggest AKAP-Lbc positions PKA for a preferred role in the phosphorylation of Ser 838 on KSR-1 to ensure activation of the ERK cascade.

We have evaluated how AKAP-Lbc shapes ERK signalling through its interaction with KSR-1. The convergence of AKAP-Lbc and KSR-1 binding partners not only generates pockets of concentrated enzyme activity that amplify mitogenic signals, but also creates a platform for cAMP-responsive modulation of the ERK cascade. Although we have not yet established the stoichiometry of the components in this network, the model presented in Figure 5v depicts AKAP-Lbc as an enhancer of RAF signalling that augments the processive phosphorylation and activation of MEK and ERK. Our biochemical and live-cell imaging experiments support this hypothesis by demonstrating that AKAP-Lbc expression levels affect the rate and amplitude of signal relay through the ERK cascade. A fundamental element of this process is the ability of AKAP-Lbc to secure RAF in proximity to its preferred substrate, MEK.

A customary trait of AKAPs is the ability to compartmentalize the PKA holoenzyme with preferred substrates[23]. Our results confirm and extend this concept by placing AKAP-Lbc at an interface between the cAMP and ERK signalling cascades, and provide a plausible explanation for evidence that indicates PKA subunits co-purify with RAF[25]. PKA phosphorylation of multiple sites on the C-Raf isoform is known to suppress signal relay to MEK[26]. Our evidence that B-Raf and C-Raf co-purify with AKAP-Lbc (Fig. 2 and Supplementary Information, Fig. S2) may have important ramifications for this process as these isozymes respond differently to cAMP. Therefore, it is tempting to speculate that AKAP-Lbc–KSR-1 networks that incorporate C-Raf may respond differently to cAMP than those that include B-Raf. This model suggests a reasonable, albeit simplistic, explanation for the longstanding conundrum that PKA activation can have both positive and negative effects on ERK activity.

Another notable feature of this work is the discovery that anchored PKA phosphorylates KSR-1 to sustain ERK signalling. These studies focus on a consensus PKA substrate site surrounding Ser 838 that is invariant in mammals and is highly conserved across species down to *Drosophila melanogaster* and *Caenorhabditis elegans* (Fig. 4d). We propose that phosphorylation of this site by PKA or related kinases is necessary to sustain a fully functional ERK signalling network as substitution of Ser 838 with alanine blunts cAMP- and growth factor-dependent activation of ERK1/2 (Fig. 5). Phosphorylation of Ser 838 in the resting state may also be favoured because the anchored PKA has preferential access to KSR-1. Thus, AKAP-Lbc may connect PKA to the ERK kinase cascade in several ways. This offers a mechanistic insight into what has long been considered to be an enigmatic cellular process: cAMP-responsive control of cell growth. □

METHODS

Methods and any associated references are available in the online version of the paper at http://www.nature.com/naturecellbiology/

Note: Supplementary Information is available on the Nature Cell Biology website

ACKNOWLEDGEMENTS

The authors wish to thank members of the Scott lab for critical evaluation of this work, M. Milnes for assistance in preparation of the manuscript, and K.L. Guan (UCSD) and R. Marais (ICR, London) for plasmids encoding KSR-1 and Flag–B-Raf. J.D.S. was supported in part by HL088366.

AUTHOR CONTRIBUTION.

F.D.S and L.K.L performed all experiments. F.D.S., L.K.L and J.D.S. designed and analysed all experiments and wrote the manuscript. T.P. performed mass spectrometry. D.K.M. generated KSR-1 rescue MEFs. R.J.D. and C.C. developed and characterized the FRET reporters.

COMPETING FINANCIAL INTERESTS

The authors declare no competing financial interests.

Published online at http://www.nature.com/naturecellbiology
Reprints and permissions information is available online at http://npg.nature.com/reprintsandpermissions/

1. Raman, M., Chen, W. & Cobb, M. H. Differential regulation and properties of MAPKs. *Oncogene* **26,** 3100–3112 (2007).
2. Mansour, S. J. *et al.* Transformation of mammalian cells by constitutively active MAP kinase kinase. *Science* **265,** 966–970 (1994).
3. Wan, P. T. *et al.* Mechanism of activation of the RAF-ERK signaling pathway by oncogenic mutations of B-RAF. *Cell* **116,** 855–867 (2004).
4. Wilhelm, S. M. *et al.* Preclinical overview of sorafenib, a multikinase inhibitor that targets both Raf and VEGF and PDGF receptor tyrosine kinase signaling. *Mol. Cancer Ther.* **7,** 3129–3140 (2008).
5. Tsai, J. *et al.* Discovery of a selective inhibitor of oncogenic B-Raf kinase with potent antimelanoma activity. *Proc. Natl Acad. Sci. USA* **105,** 3041–3046 (2008).

6. Wu, J. *et al.* Inhibition of the EGF-activated MAP kinase signaling pathway by adenosine 3', 5'-monophosphate. *Science* **262,** 1065–1072 (1993).
7. Cook, S. J. & McCormick, F. Inhibition by cAMP of ras-dependent activation of raf. *Science* **262,** 1069–1072 (1993).
8. Downward, J. Targeting RAS signalling pathways in cancer therapy. *Nat. Rev. Cancer* **3,** 11–22 (2003).
9. Stork, P. J. & Schmitt, J. M. Crosstalk between cAMP and MAP kinase signaling in the regulation of cell proliferation. *Trends Cell Biol.* **12,** 258–266 (2002).
10. Bos, J. L. Epac: a new cAMP target and new avenues in cAMP research. *Nat. Rev. Mol. Cell Biol.* **4,** 733–738 (2003).
11. Dumaz, N. & Marais, R. Integrating signals between cAMP and the RAS/RAF/MEK/ERK signalling pathways. *FEBS J.* **272,** 3491–3504 (2005).
12. Dodge-Kafka, K. L. *et al.* The protein kinase A anchoring protein mAKAP coordinates two integrated cAMP effector pathways. *Nature* **437,** 574–578 (2005).
13. Diviani, D., Soderling, J. & Scott, J. D. AKAP-Lbc anchors protein kinase A and nucleates Gα12-selective Rho-mediated stress fiber formation. *J. Biol. Chem.* **276,** 44247–44257 (2001).
14. Carnegie, G. K., Smith, F. D., McConnachie, G., Langeberg, L. K. & Scott, J. D. AKAP-Lbc nucleates a protein kinase D activation scaffold. *Mol. Cell* **15,** 889–899 (2004).
15. Therrien, M., Michaud, N. R., Rubin, G. M. & Morrison, D. K. KSR modulates signal propagation within the MAPK cascade. *Genes Dev.* **10,** 2684–2695 (1996).
16. Harvey, C. D. *et al.* A genetically encoded fluorescent sensor of ERK activity. *Proc. Natl Acad. Sci. USA* **105,** 19264–19269 (2008).
17. Leevers, S. J., Paterson, H. F. & Marshall, C. J. Requirement for Ras in Raf activation is overcome by targeting Raf to the plasma membrane. *Nature* **369,** 411–414 (1994).
18. Muller, J., Ory, S., Copeland, T., Piwnica-Worms, H. & Morrison, D. K. C-TAK1 regulates Ras signaling by phosphorylating the MAPK scaffold, KSR1. *Mol. Cell* **8,** 983–993 (2001).
19. Scott, J. D. & Pawson, T. Cell signaling in space and time: where proteins come together and when they're apart. *Science* **326,** 1220–1224 (2009).
20. Morrison, D. K. & Davis, R. J. Regulation of MAP kinase signaling modules by scaffold proteins in mammals. *Annu. Rev. Cell Dev. Biol.* **19,** 91–118 (2003).
21. Bhattacharyya, R. P., Remenyi, A., Yeh, B. J. & Lim, W. A. Domains, motifs and scaffolds: the role of modular interactions in the evolution and wiring of cell signaling circuits. *Annu. Rev. Biochem.* **75,** 655–680 (2006).
22. Matheny, S. A. *et al.* Ras regulates assembly of mitogenic signalling complexes through the effector protein IMP. *Nature* **427,** 256–260 (2004).
23. Smith, F. D., Langeberg, L. K. & Scott, J. D. The where's and when's of kinase anchoring. *Trends Biochem. Sci.* **31,** 316–323 (2006).
24. Nguyen, A. *et al.* Kinase suppressor of Ras (KSR) is a scaffold which facilitates mitogen-activated protein kinase activation *in vivo*. *Mol. Cell Biol.* **22,** 3035–3045 (2002).
25. Dumaz, N. & Marais, R. Protein kinase A blocks Raf-1 activity by stimulating 14-3-3 binding and blocking Raf-1 interaction with Ras. *J. Biol. Chem.* **278,** 29819–29823 (2003).
26. Dhillon, A. S. *et al.* Cyclic AMP-dependent kinase regulates Raf-1 kinase mainly by phosphorylation of serine 259. *Mol. Cell Biol.* **22,** 3237–3246 (2002).

DOI: 10.1038/ncb2130

METHODS

Cells and reagents. HEK293, NIH3T3 and KSR-1 MEF cells were cultured in Dulbecco's Modified Eagle Medium (DMEM) supplemented with 10% (v/v) fetal bovine serum (FBS) and penicillin/streptomycin. Where indicated cells were treated with 10 ng ml^{-1} EGF. Cells were transfected overnight using Transit-LT1 (Mirus) for plasmids or with Dharmafect 1 (Dharmacon) for siRNA oligonucleotides. The plasmid encoding HA–mKSR1 was provided by K.L. Guan (University of California, USA). Mutations were introduced using the Quickchange XL kit (Stratagene). Plasmids encoding Flag–c-Raf and Flag–B-Raf were provided by R. Marais (ICR, London). siRNA oligonucleotides for AKAP-Lbc were 5′-GTGCGTCTCAATGAGATTT-3′ or 5′-GCATATTGCTTGTAACTCA-3′, All other chemicals were from Sigma or EMD.

Antibodies and dilutions. The following antibodies were used in this study: anti-KSR-1 monoclonal antibody (BD 611576; 250 ng ml^{-1}), anti-AKAP-Lbc (V096; 1 μg ml^{-1}), anti-total MAPK (Cell Signalling Technology 9102; 1:500), anti-phospho-ERK1/2 (Cell Signalling Technology 9101; 1:500), anti-phospho-MEK1/2 (Millipore 05-747; 1:500), anti-MEK1/2 (Cell Signalling Technology 9126; 1:500) anti-B-Raf (Santa Cruz Biotechnology SC-5284; 200 ng ml^{-1}), anti-PKAc (BD 610989; 250 ng ml^{-1}), anti-PKA RIIα (BD 612243; 250 ng ml^{-1}), anti-PKA RIIβ (BD 610626; 250 ng ml^{-1}), anti-HA (Sigma H9658; 1:2,000 or Sigma H6533; 1:1,000), anti-Flag (Sigma F1804; 1 μg ml^{-1} or Sigma A8592; 1:1,000), anti-GFP (Invitrogen A11122; 1:1,000 or Santa Cruz Biotech SC-9996; 200 ng ml^{-1}; anti-Myc (Santa Cruz Biotech SC-789; 200 ng ml^{-1}) and anti-pyo (D.K.M.; 1:1,000). The majority of western blot data was collected using an Alpha Innotech MultiImage III with FluoroChemQ software.

Cell treatment and lysis. Cells were washed in cold PBS and harvested 36–48 h post-transfection in Tris lysis buffer (25 mM Tris at pH 7.5, 150 mM NaCl, 1% (v/v) Triton X-100, 0.5 mM MgCl2, 1 mM EDTA, 1 mM EGTA, 1 mM NaVO3, 20 mM NaF, 100 nM okadaic acid and protease inhibitors). Lysates were centrifuged at 19,400*g* (Eppendorf 5417R) for 20 min at 4 °C. For some experiments, cells were starved for 12–16 h in DMEM, supplemented with 0.1% (v/v) bovine serum albumin (BSA) before treatment. For stimulation of cAMP production and PKA activity, cells were treated with 10 μM H-89 for 30 min before treatment with a cocktail of forskolin and IBMX (20 μM and 75 μM final, respectively) for 10 min at 37 °C and harvesting.

Recombinant protein production. Plasmids encoding GST fusion proteins of AKAP-Lbc fragments[14] were transformed into BL21(DE3)pLysS bacteria. Protein expression was induced by addition of 1 mM isopropyl-1-thio-β-D-galactopyranoside and overnight growth at 30 °C. Fusion proteins were either purified in large batches using glutathione–Sepharose (GE Life Sciences), or induced bacteria were frozen in small aliquots and proteins were purified at the time of the experiment. For some experiments, protein was produced *in vitro* using a T7 TNT kit (Promega).

Cell staining. NIH3T3 cells and MEFs were cultured on glass coverslips (no. 1.5). Cells were fixed with 4% (v/v) paraformaldehyde in PBS for 20 min at room temperature, permeabilized in PBS (supplemented with 0.2% (w/v) BSA and 0.1% (v/v) Triton X-100) for 10 min, and stained with the appropriate primary antibodies overnight at 4 °C. Cells were washed three times in PBS and incubated with Alexa Fluor conjugated secondary antibodies (1:500) for 2 h at room temperature. Cells were washed again and mounted on glass slides using ProLong antifade media (Invitrogen). Nuclei were stained with DRAQ5 or DAPI (4',6-diamidino-2-phenylindole) in the final step before mounting. Cells were imaged with either a Zeiss LSM 510 META or a Zeiss AxioObserver microscope with an Apotome slider.

***In vitro* phosphorylation.** After immunoprecipitation and washing, immunocomplexes were washed once in PKA assay buffer (40 mM Tris at pH 7.5, 10 mM MgOAc, 0.1 mM EGTA and 0.05 mM ATP). Phosphorylation reactions were performed in assay buffer for 10–30 min at 30 °C. Assays were supplemented with PKA C-subunit (0.2 μg) or cAMP (0.1 mM). PKI (10 μM final) was included in some reactions to block kinase activity. Reactions were stopped by addition of 2 × NuPAGE sample buffer (Invitrogen) and were analysed by SDS–PAGE and autoradiography. Peptide arrays were produced by SPOT synthesis with a MultiPep robot (Intavis AG). Membranes were blocked in PKA assay buffer containing 100 μM ATP, and phosphorylated as above. After extensive washing, membranes were dried and exposed to film for autoradiography.

Immunoprecipitated-complex kinase assays. B-Raf activity in immunocomplexes was measured using the Raf kinase assay kit for chemiluminescence detection from Millipore (#17-360). The inhibitors sorafenib (Symansis) and ZM336572 (Tocris) were included where appropriate at 1 μM and 10 μM, respectively.

Mass spectrometry. HEK293 cells were transfected with plasmids expressing Flag–AKAP-Lbc. After lysis, immunocomplexes were isolated using Flag–M2 agarose (Sigma) and separated by SDS–PAGE on 4–12% (w/v) NuPAGE gels (Invitrogen). Gels were stained with GelCode Blue (Thermo-Pierce) and bands were excised. Proteins were identified as described[27].

FRET measurements. HEK293 cells were cultured on 35-mm dishes with poly-D-lysine coated glass coverslip bottoms (MatTek Corporation). Cells were transfected with plasmids encoding the cerulean (CFP)/venus (vYFP) variants of $EKAR_{cyto}$ and $EKAR_{nuc}$[16] along with appropriate vectors (see figure legends). For siRNA experiments, siRNA oligonucleotides were transfected 1 day before transfection with EKAR constructs. After starving overnight, cells were placed in EKAR recording solution (25 mM HEPES at pH 7.4, 114 mM NaCl, 2.2 mM KCl, 2 mM $CaCl_2$, 2 mM $MgCl_2$, 22 mM $NaHCO_3$, 1.1 mM NaH_2PO_4 and 2 mM glucose). Fluorescence emission was acquired using a DMI6000B inverted microscope (Leica), an EL6000 microscope (fluorescent light source, filter wheel, ultra fast shutter, Leica) and a CoolSnap HQ camera (Photometrics) all controlled by MetaMorph 7.6.4 (Molecular Devices). Dual-emission images were obtained simultaneously through a Dual-View image splitter (Photometrics) with S470/30 and S535/30 emission filters and 505 dcxr dichroic mirror (Chroma). Exposure time was 200 ms with an image interval of 20 s. FRET changes within a region of interest were calculated as the ratio of measured fluorescent intensities from two channels (M_{donor}, $M_{indirectAcceptor}$) after subtraction of background signal. FRET ratio (YFP/CFP) changes after ERK activation by EGF (0.1 μg ml^{-1}) and MEK inhibition by UO126 (10 μM) are normalized to the average FRET ratio value before stimulation. Where indicated, cells were pre-treated with 10 μM st-Ht31 peptide (Promega) for 30 min before FRET recording.

Statistical analyses. Analyses were performed using Graph Pad Prism. All data are expressed as mean ± s.e.m. Differences were examined by one-way analysis of variance (ANOVA) or paired *t*-test. A P value < 0.05 was considered significant, and a P value < 0.01 was considered very significant.

Pulldowns and immunoprecipitations. These experiments were performed as in ref. 27

27. Jin, J. *et al.* Proteomic, functional, and domain-based analysis of *in vivo* 14-3-3 binding proteins involved in cytoskeletal regulation and cellular organization. *Curr. Biol.* **14,** 1436–1450 (2004).

nature cell biology

DOI: 10.1038/ncb2130

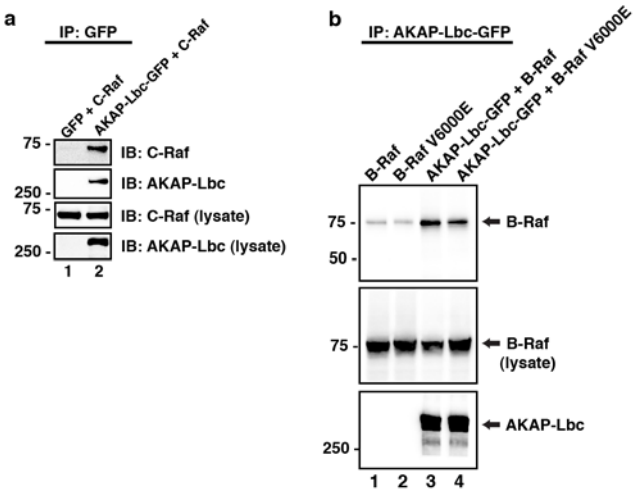

Figure S1 AKAP-Lbc interacts with C-Raf and the oncogenic B-Raf V600E mutant. **(a)** HEK293 cells were transfected with plasmids encoding FLAG-C-Raf and AKAP-Lbc-GFP or GFP alone. Immune complexes were isolated using anti-GFP antibodies and associated C-Raf (top) and AKAP-Lbc were detected by immunoblotting with anti-FLAG-HRP. Control immunoblots show the levels of both proteins in cell lysates **(b)** HEK293 cells were transfected with plasmids encoding FLAG-B-Raf or FLAG-B-Raf V600E alone or with AKAP-Lbc-GFP. Immune complexes were isolated using anti-GFP antibodies and associated B-Raf (top) was detected by immunoblotting. Control immunoblots show the levels of both proteins in cell lysates

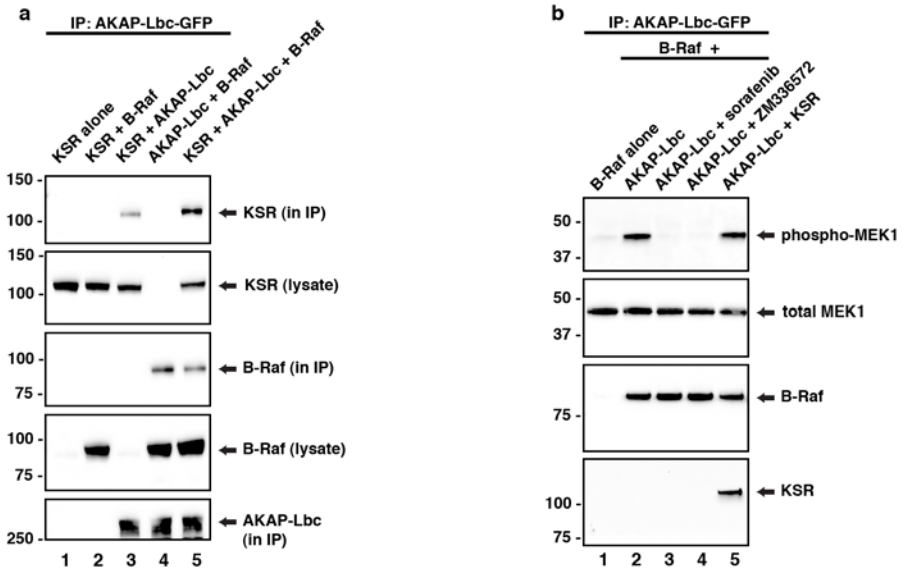

Figure S2 Analysis of AKAP-Lbc-KSR-B-Raf complexes. **(a)** KSR-1, B-Raf and AKAP-Lbc were expressed in HEK293 cells in various combinations. Immunocomplexes were isolated using anti-GFP antibodies and associated KSR-1 and B-Raf were detected by immunoblotting. B-Raf expression increases the amount of KSR-1 found in AKAP-Lbc complexes. **(b)** Effect of KSR-1 expression on AKAP-Lbc associated B-Raf activity. B-Raf activity in AKAP-Lbc complexes was measured as in Figure 2. KSR-1 expression has no effect on B-Raf activity in IPs (lanes 2 & 5). The B-Raf inhibitors sorafenib and ZM336572 were used as controls for specificity of the kinase assay (lanes 3 & 4).

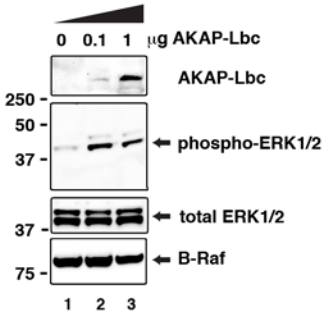

Figure S3 AKAP-Lbc stimulates ERK1/2 activity in non-starved cells. HEK293 cells were transfected with vectors encoding HA-MEK1 and FLAG-B-Raf along with increasing amounts of AKAP-Lbc-GFP plasmid. AKAP-Lbc, phospho-ERK1/2, total MEK, and B-Raf were detected by immunoblotting.

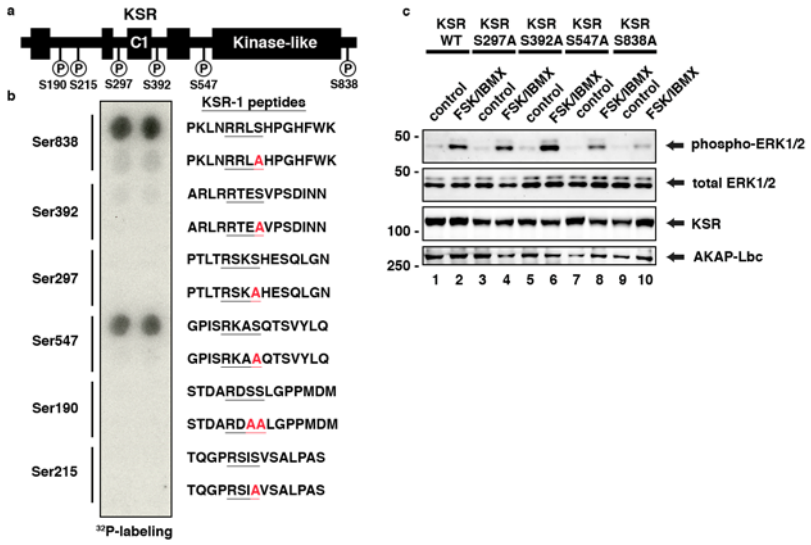

Figure S4 Analysis of KSR-1 phosphorylation by PKA. **(a)** Scansite (http://scansite.mit.edu/) was used to predict potential PKA phosphorylation sites in KSR-1 (schematic). **(b)** Immobilized peptides corresponding to these sites were produced by SPOT synthesis. Membranes were incubated PKA and ^{32}P-ATP for 30 min at 30ºC and phosphorylation was detected by autoradiography. **(c)** Several potential PKA sites, including 14-3-3 binding sites (S297 and S392) and sites identified in (b) (S547 and S838) were mutated to alanine and tested for effects on cAMP stimulated ERK1/2 activation. Levels of phospho-ERK1/2, total ERK1/2, KSR-1 and AKAP-Lbc were detected by immunoblotting.

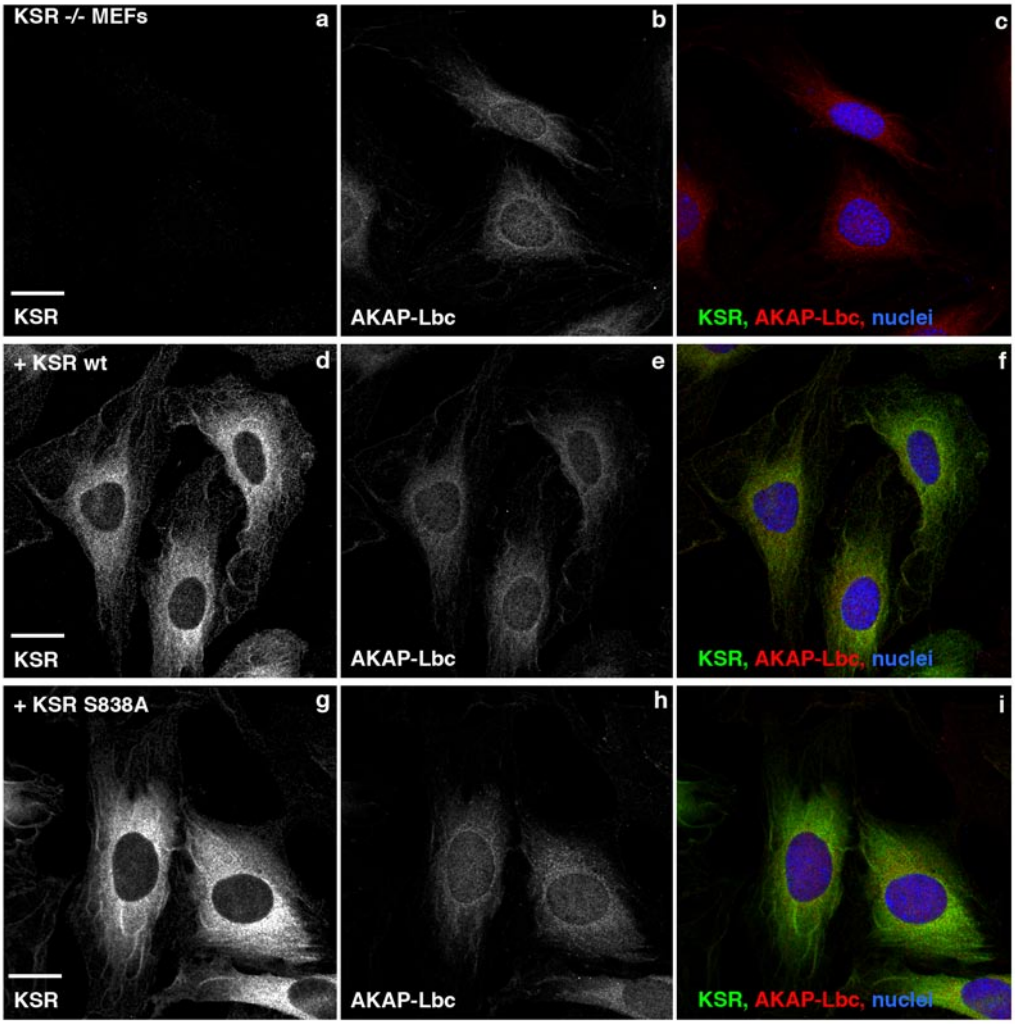

Figure S5 Expression of KSR-1 and AKAP-Lbc in mouse embryonic fibroblast cell lines. KSR -/- MEFs and MEFs re-expressing WT KSR-1 or KSR-1 S838A were fixed and stained for Immunofluorescence with antibodies against KSR-1 and AKAP-Lbc. Nuclear DNA was visualized by co-staining with DRAQ5. **(a, d & g)** KSR is expressed at similar levels in the WT and S838A rescue cells and is absent in KSR -/- cells. **(b, e & h)** AKAP-Lbc is present in all three cell lines. **(c, f & i)** Composite images. Scale bars represent 20 μm.

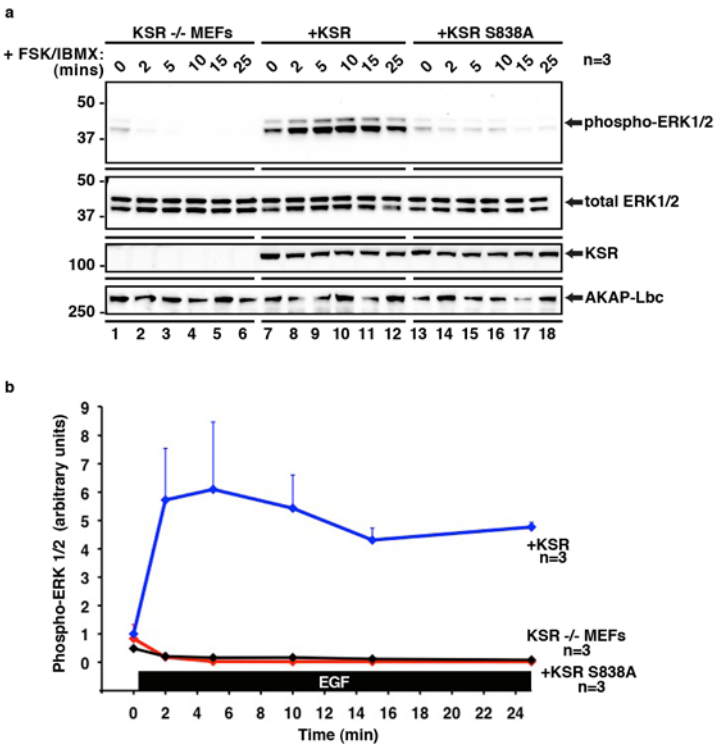

Figure S6 Time course of ERK1/2 activation in response to cAMP in KSR MEF lines. **(a)** KSR -/- MEFs and MEFs re-expressing WT KSR-1 or KSR-1 S838A were treated with 20 μM forskolin and 75 μM IBMX for the times indicated. Lysates were separated by SDS-PAGE and phospho-ERK1/2, ERK1/2, KSR-1 and AKAP-Lbc were detected by immunoblotting. Increasing cAMP activates ERK1/2 in MEFs expressing WT KSR-1, but not in cells expressing KSR-1 S838A or in cells lacking KSR-1. **(b)** Graph depicting quantitation of ERK 1/2 phosphorylation in KSR-1 -/- MEFs (red diamonds), WT KSR-1 rescued MEFs (blue diamonds) and KSR-1 S838A MEFs (black diamonds) by densitometry (mean ± SEM).

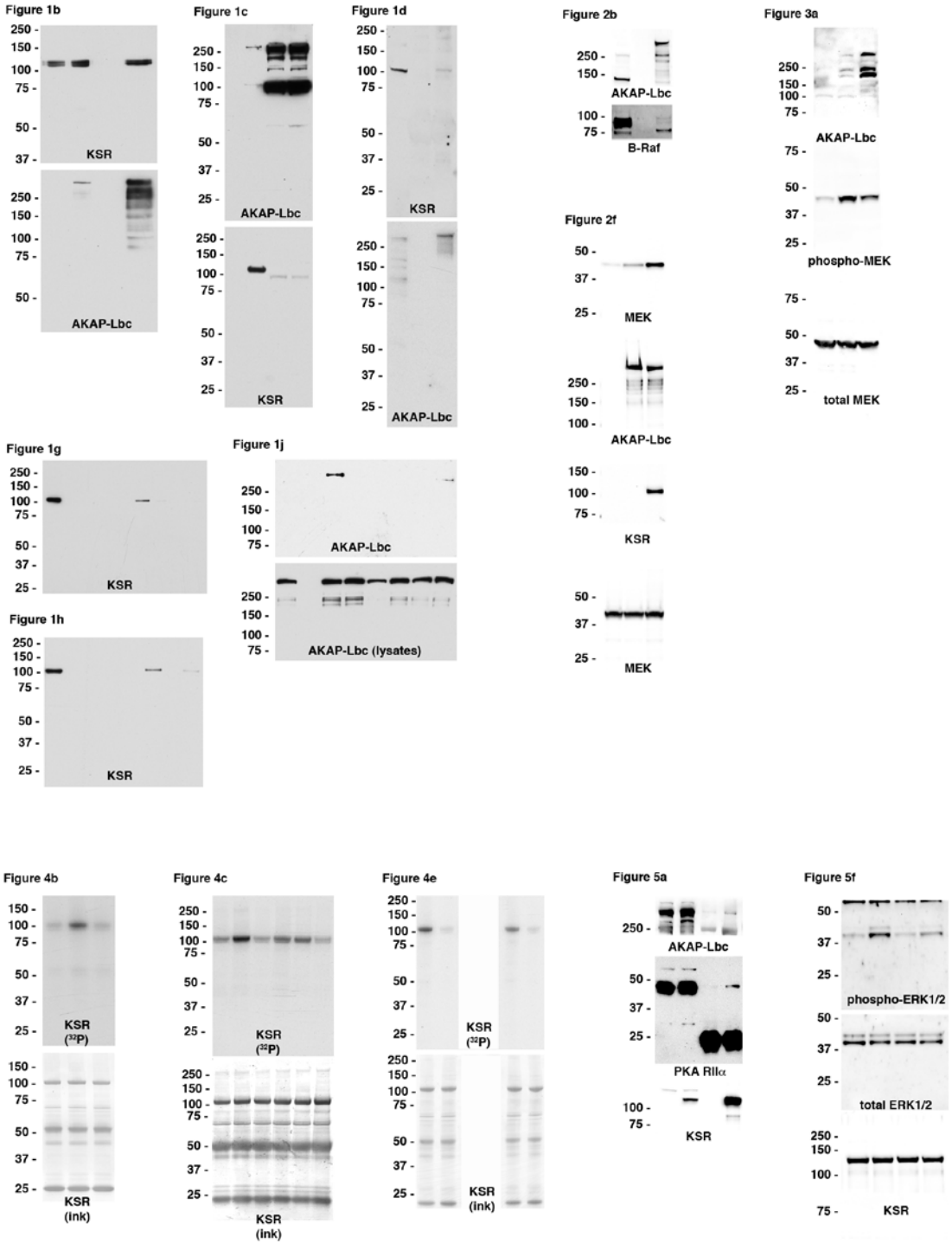

Figure S7 Full scans of key gel/western blot data. Blots not shown here were cut into strips and probed for specific antigens. The data in the figures represents the area of the blot used for each experiment. Molecular weight markers are included in the main figures.